Design Proposal of a Metal Detector for Humanitarian Demining

John Fernando Vargas Buitrago[*1], Yarien Moreno[*2], Roberto Bustamante Miller[#3]
*Universidad Pontificia Bolivariana, Medellín - Colombia,
1. johnfdo.vargas@upb.edu.co
2.yarien.moreno@up.ac.pa
#Universidad de los Andes, Bogotá – Colombia (111711)
3.rbustama@uniandes.edu.co

***Abstract*—In this research work, a novel design of a metal detector is proposed. To fulfill this, several results obtained with an edge based FEM simulator, and an analytical model were used.**

The main objective of the proposed detector is to diminish the influence of the soil in the detector performance, given that this is an important problem on landmine detection[1]. By using numerical modeling could be demonstrated the feasibility of the proposed design.

Keywords: Demining,Electromagnetic fields, Humanitarian demining, Landmines, Metal detectors, Numerical modeling.

I. INTRODUCTION

According to [2] a receiver coil will get the field induced directly by the transmitter coil, the field induced by the soil and the field induced by buried objects. Usually, a metal detector senses the sum of those induced fields and it should discern the presence of a metal from the mix of fields[2].

The field induced directly by the transmitter coil on the receiver coil could be excluded from the measure; given that, it generates a constant voltage. Commonly, this voltage is measured during the detector construction, and it is defined as a threshold or zero reference level, it could require periodic calibration and it could show important problems when the battery is discharging.

By other side, it is necessary to recognize the signal produced by soil, the soil itself induces a voltage in the receiver coil that could be construed as the presence of a metal. Usually it is necessary to do some calibration procedures with commercial detectors, before the detection process is made; however, soil can show variable electromagnetic properties and the detector would work decalibrated.

II. METHODS

The influence of soils in metal detector performance has been studied previously. Theoretically, by using analytical models in [2] ,[3] y [4], by using a numerical modeling. These studies, allow to conclude that the electromagnetic properties of soils are highly influent in the detector performance, especially when soils have relative magnetic permeability different from 1. It was experimentally confirmed in [1], these results show that a detector can decrease its probability of detection and increase its false alarms rate, when the soil is magnetic. Taking into consideration that a detector needs a strategy to diminish the effect of soil in its performance.

In order to calculate the induced field of a buried metal a finite elements simulator was developed. In this simulator the model presented in [6] was implemented using the Matlab software

This design proposal aims to vanish the voltage induced directly by the transmitter coil, and the voltage induced by soil, in order to avoid a pair of calibrations.

To fulfill this, it is needed to analyze the induced magnetic fields behavior in the scenario of Fig.1, a horizontal coil over a half space.

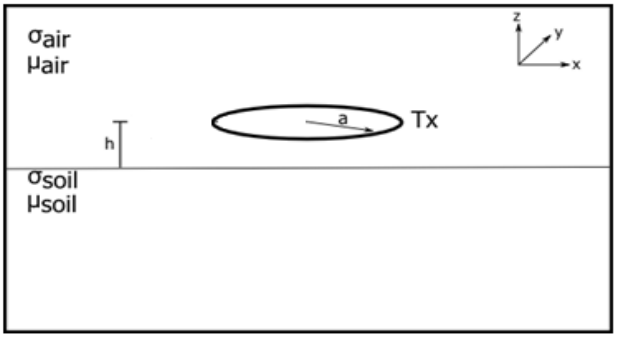

Fig.1. Horizontal coil over a homogeneous soil.

The magnetic field induced by the coil in the air (Fig.1) at the ρ, z position can be calculated with the equations (1), (2), (5) and (6), and the magnetic field induced by the homogenous soil under a variable magnetic field produced by an horizontal transmitter coil, could be calculated with equations (3), (4), (7) and (8):

If$z > h$

$$H_{0\rho}^{air} = \frac{Ia}{2}\int_0^{\infty} \lambda J_1(\lambda a) J_1(\lambda \rho)\left(e^{-\lambda(z-h)}\right)d\lambda \quad (1)$$

$$H_{0z}^{air} = \frac{Ia}{2}\int_0^{\infty} \lambda J_1(\lambda a) J_0(\lambda \rho)\left(e^{-\lambda(z-h)}\right)d\lambda \quad (2)$$

$$H_{0\rho}^{soil} = \frac{Ia}{2}\int_0^{\infty} \frac{\mu_{soil}u_o - \mu_o u_1}{\mu_{soil}u_o + \mu_o u_1} J_1(\lambda a) J_1(\lambda \rho) e^{-\lambda(z+h)} d\lambda \hat{\phi} \quad (3)$$

$$H_{0z}^{soil} = \frac{Ia}{2}\int_0^{\infty} \frac{\mu_{soil}u_o - \mu_o u_1}{\mu_{soil}u_o + \mu_o u_1} J_1(\lambda a) J_0(\lambda \rho) e^{-\lambda(z+h)} d\lambda \hat{\phi} \quad (4)$$

if$0 < z < h$

$$H_{0\rho}^{air} = -\frac{Ia}{2}\int_0^{\infty} \lambda J_1(\lambda a) J_1(\lambda \rho)\left(e^{-\lambda(h-z)}\right)d\lambda \quad (5)$$

$$H_{0z}^{air} = \frac{Ia}{2}\int_0^{\infty} \lambda J_1(\lambda a) J_0(\lambda \rho)\left(e^{-\lambda(h-z)}\right)d\lambda \quad (6)$$

$$H_{0\rho}^{soil} = \frac{Ia}{2}\int_0^{\infty} \frac{\mu_{soil}u_o - \mu_o u_1}{\mu_{soil}u_o + \mu_o u_1} J_1(\lambda a) J_1(\lambda \rho) e^{-\lambda(h+z)} d\lambda \hat{\phi} \quad (7)$$

$$H_{0z}^{soil} = \frac{Ia}{2}\int_0^{\infty} \frac{\mu_{soil}u_o - \mu_o u_1}{\mu_{soil}u_o + \mu_o u_1} J_1(\lambda a) J_0(\lambda \rho) e^{-\lambda(h+z)} d\lambda \hat{\phi} \quad (8)$$

Where

${u_o}^2 = \lambda^2 + {k_o}^2,\ {u_1}^2 = \lambda^2 + {k_1}^2$

${k_o}^2$=0 *(In the quasi static domain)*

${k_1}^2 = i\sigma_{soil}\mu_{soil}\omega$ *(In the quasi static domain)*

$\mu_0 is magnetic permability of free space = 4x10^{-7}\frac{H}{m}$

$\mu_{soil} = magnetic permability of soil\ (H/m)$

$\omega = Frequency of current flowing through the trajnsmitter\left(\frac{Rad}{s}\right)$

$J_1(x) = Besselfunctions of the first kind and first order$

$a = Coil transmitter radius(m)$

$b = Coil receiver radius(m)$

$I = Current amplitude(A)$

$N_t = Number of spires in the transmitter coil$

$\lambda = Integration variable$

III. RESULTS

Since one of the main objectives of this design proposal is to vanish the voltage induced directly by the coil transmitter, a good choice is to place the receiver coil perpendicularly to the transmitter coil. According to Fig.2, the induced field in Z direction by the transmitter coil will not be sensed, given that no magnetic field lines pass through the receiver loop.

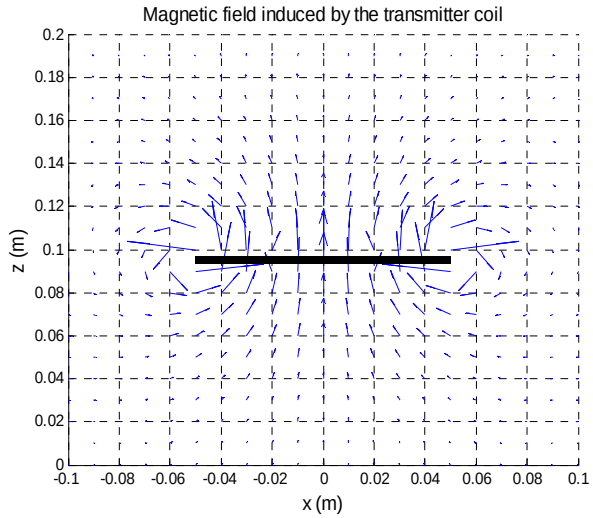

Fig.2. Induced magnetic field by the transmitter coil in the air, plane Y=0 (X-Z view).

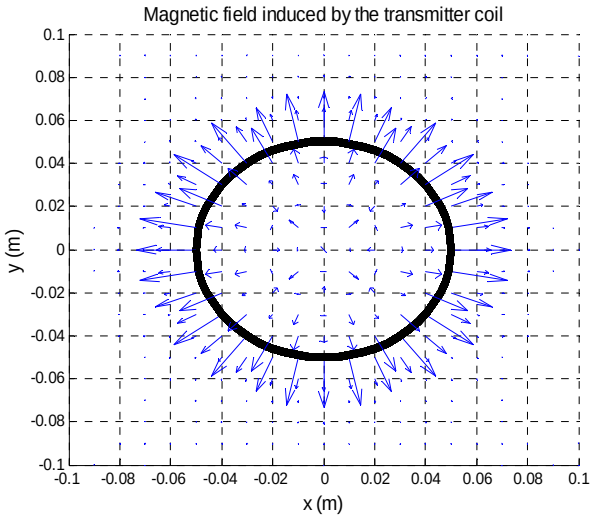

Fig.3. Induced magnetic field by the transmitter coil in the air, plane Z=h (X-Y view).

Whereas Fig.3 shows that the induced magnetic field in X and Y direction is zero if the receiver coil is placed exactly in the middle and perpendicularly to the transmitter coil (Fig.4). If the receiver coil is placed at the plane X=0, the receiver coil would sense the field in direction X, but there is not a component of the induced magnetic field in X (Fig.5), the induced field only has component in Z direction, and it does not cross the receiver coil.

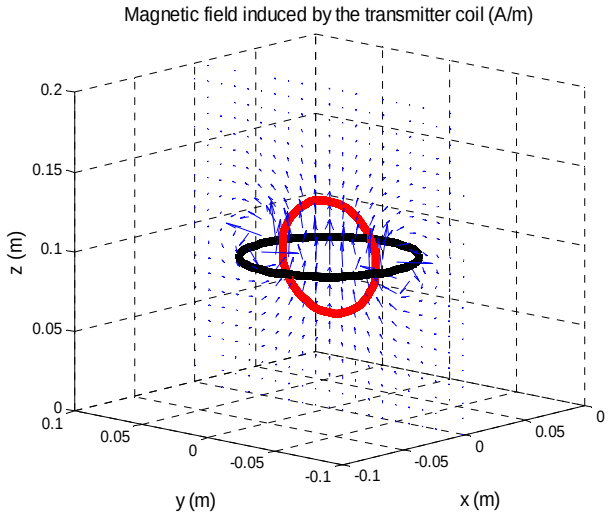

Fig.4. Receiver coil placed in plane X=0.

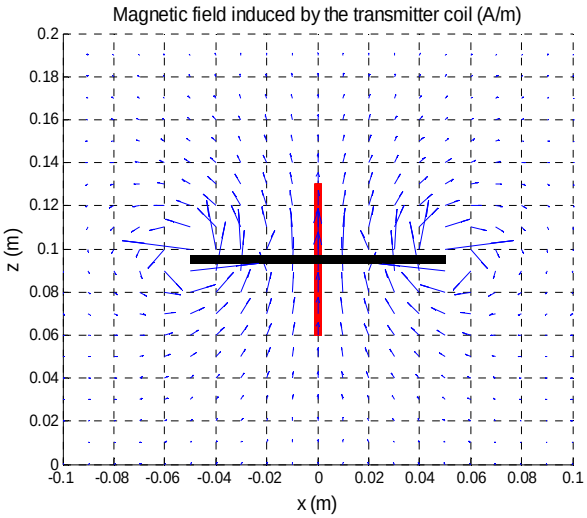

Fig.5. Induced magnetic field by the transmitter coil in the air, plane Y=0 (X-Z view).

This configuration makes it possible to eliminate the field induced by the transmitter coil, and additionally, it works well to eliminate the induced field by an homogenous soil and soil calibration could be avoided. The following figures show the magnetic field induced by a soil when it is excited by a horizontal coil.

From Fig.6 toFig.8, it can be seen that the field lines in Z direction will not be sensed by a receiver coil located in plane X=0, and the field lines in X direction will overlap cancelling each other.

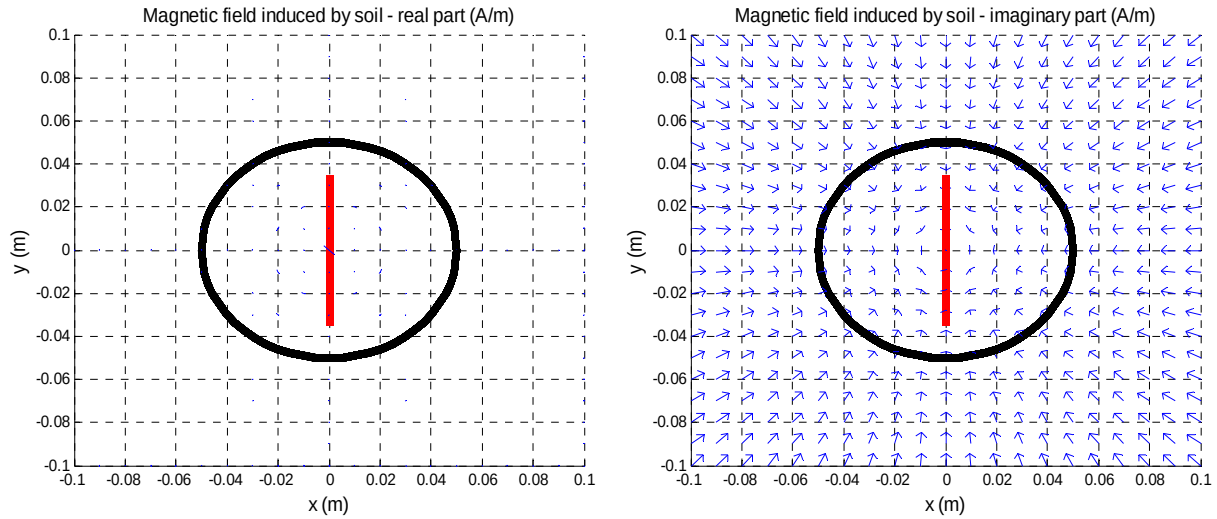

Fig.6. Real and imaginary part of the magnetic field induced by the soil, plane Z=h (X-Y view).

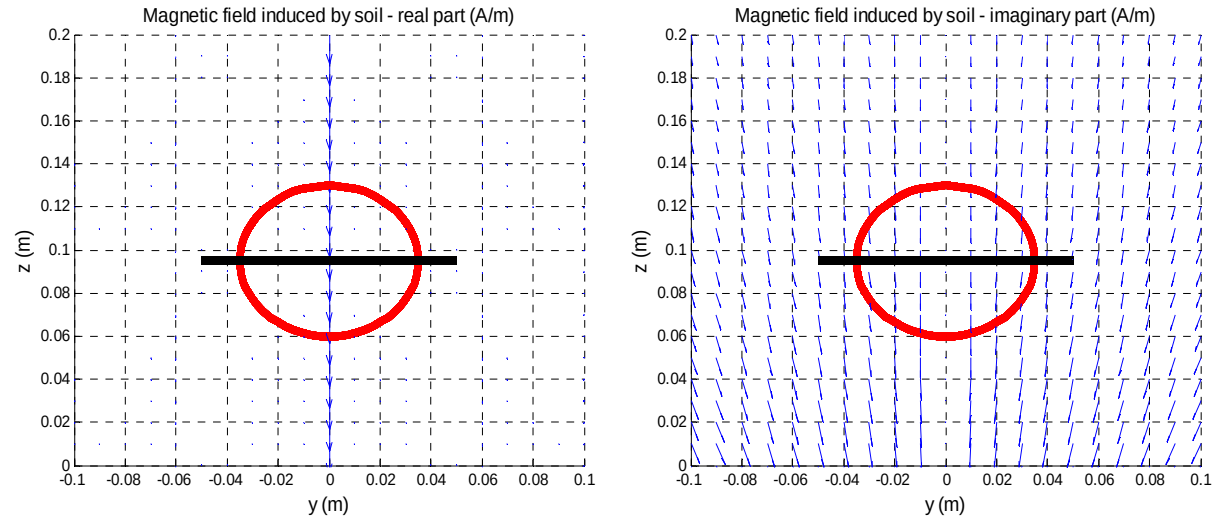

Fig.7. Real and imaginary part of the magnetic field induced by the soil, plane X=0 m (Y-Zview).

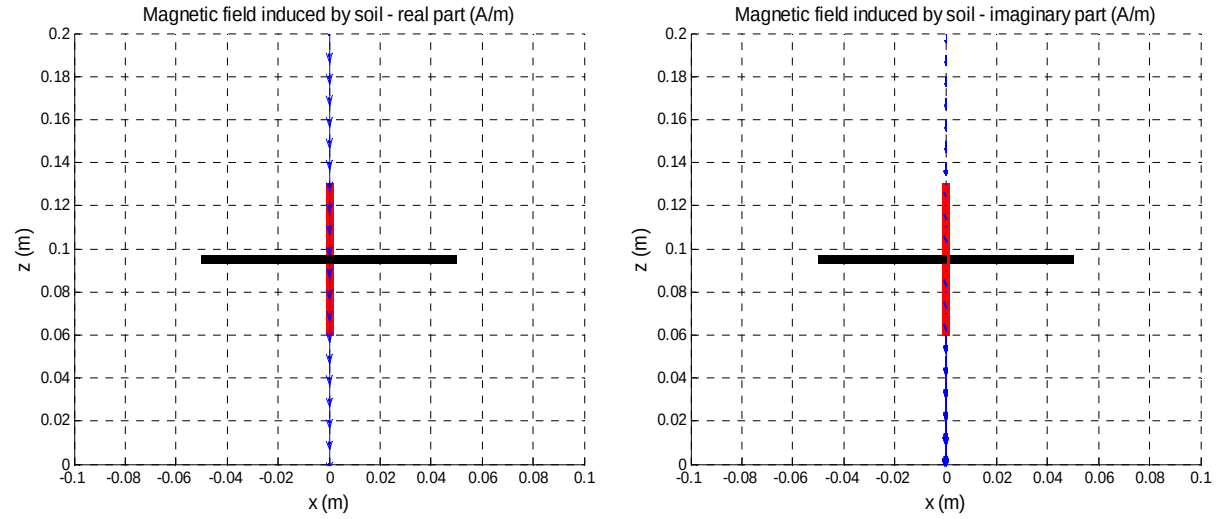

Fig.8. Real and imaginary part of the magnetic field induced by the soil, plane X=0 m (X-Zview).

Last results allow to observe that a receiver coil placed in plane X=0, above or below the transmitter coil, will not sense the field induced by the soil and the transmitter coil (Fig.9, Fig.10). Even, this condition is kept if instead of a receiver coil, several receiver coils are placed in the plane X=0 m (Fig.11, Fig.12).

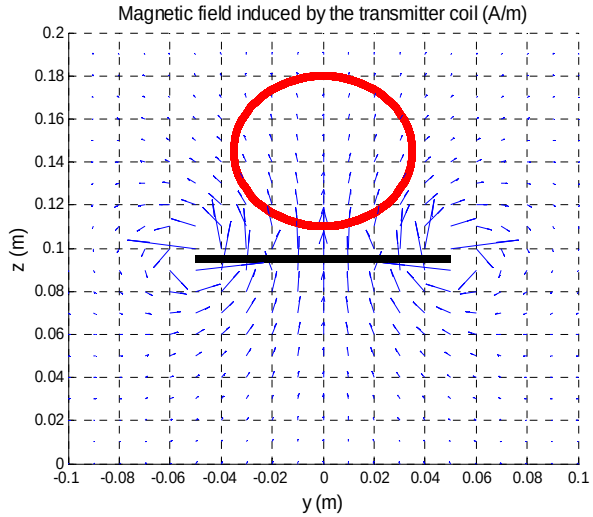

Fig.9. Receiver coil above the transmitter coil in plane X=0 m (Y-Z view).

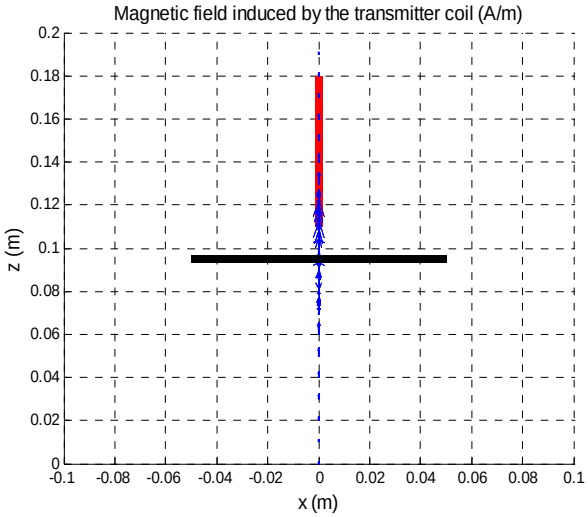

Fig.10. Receiver coil above the transmitter coil in plane X=0 m (X-Z view).

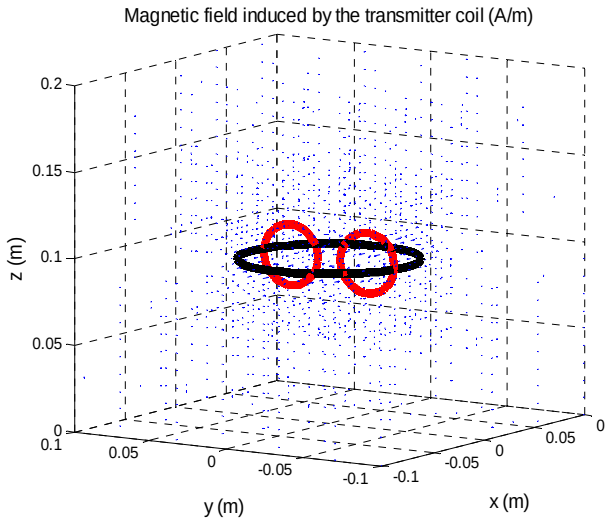

Fig.11. Two receiver coils placed in plane X=0 m.

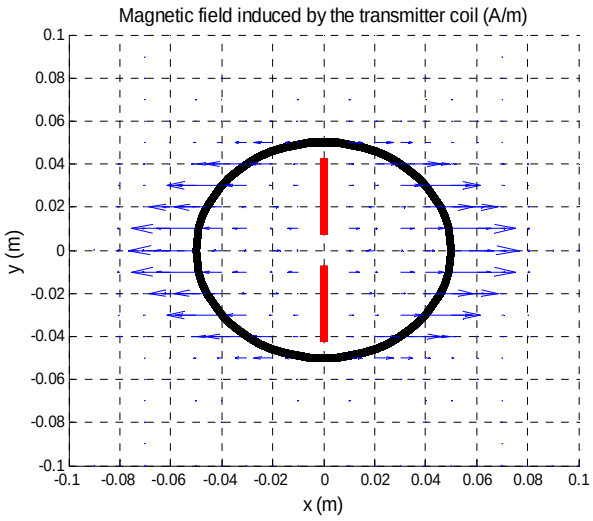

Fig.12. Magnetic field induced by the transmitter coil in X direction, two receiver coils placed in plane X=0 m (X-Y view).

The distribution of coils proposed avoid the fields induced by the soil and the transmitter coil to be measured. However, it has not been defined if it is feasible to detect buried metals. The detection is feasible in case that the buried metal generates magnetic field lines in direction X crossing the receiver coil. According to the results obtained, these field lines were effectively generated. Nonetheless, in order to analyze the detection feasibility in greater depth, another set of simulations was made, using the edge based numerical model.

The greatest magnitude of the magnetic field in X direction, appears when the center of the transmitter coil has not reached the buried target position. Therefore, it is arbitrarily assigned X=-0,02 m as the transmitter location and the plane where the receiver is placed, to get the results of Fig.13 and the subsequent figures.

Fig.13 describes the imaginary and the real part of the magnetic field induced in X direction by a metallic cube, that is buried in a non-magnetic, conductive soil (0,01 S/m), and is exposed to a variable magnetic field, generated by a 5 cm radius transmitter coil powered by a 1 A current at 50 kHz.

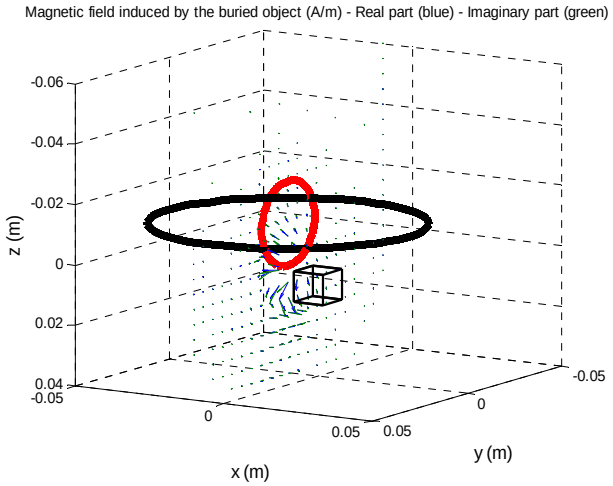

Fig.13. Induced magnetic field by a buried metallic cube in the plane X=-0,02 m - receiver coil (red).

The following figures (Fig.14–Fig.16) show the magnitude of the magnetic field induced by the buried cube, which cross the receiver located in the middle of transmitter coil. These results allow to conclude that there is indeed an induced magnetic field in X direction that could be sensed to detect a buried target, and therefore this design propose is feasible for a metal detector.

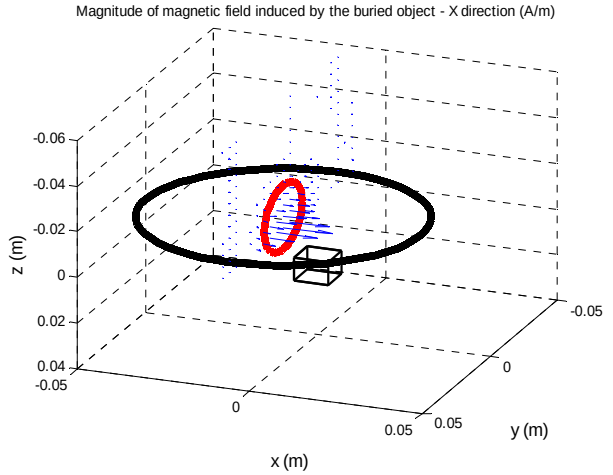

Fig.14. Magnitude of the magnetic field induced in X direction by the buried object in the plane X=-0,02 m; Z<0 - receiver coil (red).

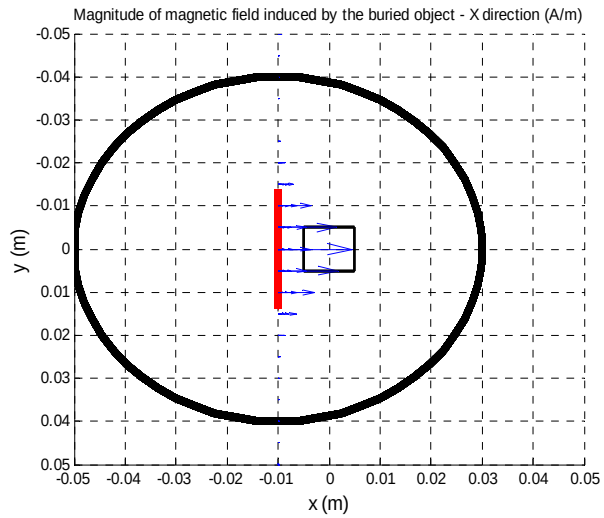

Fig.15. Magnitude of the magnetic field induced in X direction by the buried object in the plane X=-0,02 m; Z<0 (X-Y view) - receiver coil (red).

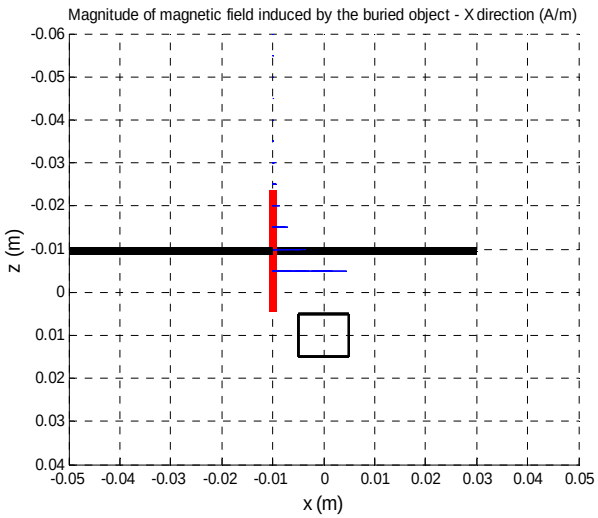

Fig.16. Magnitude of the magnetic field induced in X direction by the buried object in the plane X=-0,02 m; Z<0 (X-Z view) - receiver coil (red).

In accordance with the results previously obtained, it is feasible to detect buried metal, by placing the receiver coil perpendicularly to the transmitter coil. This detector senses the magnetic field induced by the buried object in X direction and avoids the magnetic field induced by the soil and transmitter coil.

The following results, show the behavior of the magnetic field induced in X direction, as a function of the height of the coils, in order to establish the optimal receiver location.

Fig.17 shows, how the induced magnetic field in X direction, decreases when the transmitter coil height increases, assuming that the receiver is located at the same height of the transmitter.

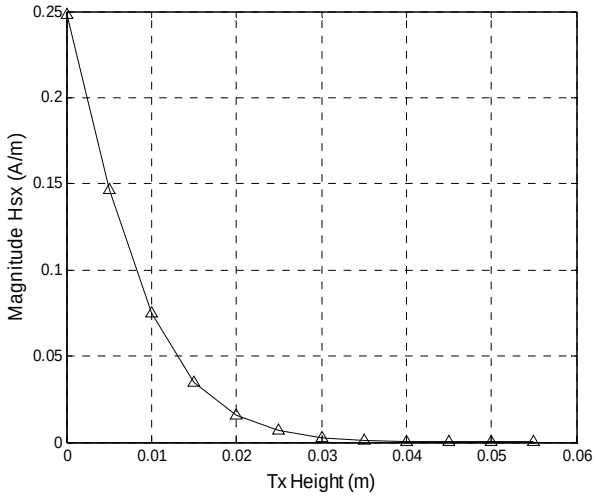

Fig.17. Transmitter coil height vs magnitude of the induced magnetic field in X direction.

Clearly, when the height of the transmitter and the receiver becomes higher, the induced magnetic field decreases, it suggests that the transmitter and receiver coils should be as close to the soil as possible. It excludes the configuration of the next figure because the transmitter coil needs to be as high as the radius of the receiver coil.

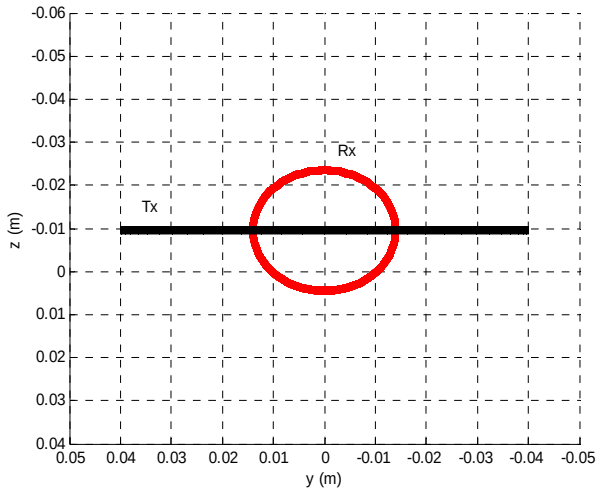

Fig.18. Possible system configuration.

Considering the above, it is proposed to use receiver coils with a flat side (Fig.19) instead of a circular coil, seeking to keep transmitter and receiver coils very close to the soil.

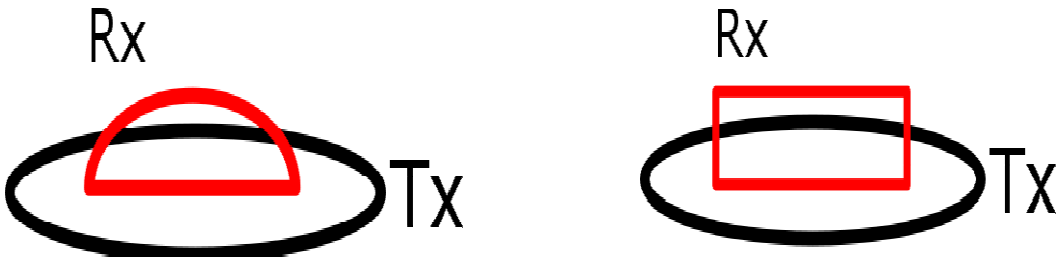

Fig.19. Proposed receiver coils.

The dimensions of the receiver coil, can be established with the objective of maximizing the voltage induced by the buried object in the receiver coil. To do this, it is needed to use the induction Faraday's law:

$$V = -N_R \frac{d\phi}{dt} \quad (9)$$

Where V is the induced voltage in a N_r turns coil, and ϕ is the magnetic flux that pass through the coil. In the frequency domain, last equation is written as:

$$V = -N_R(j\omega\Phi) \quad (10)$$

Equation (10), suggest that the higher the frequency and number of turns, the higher the induced voltage in the receiver coil.

The magnetic flux Φ that cross a surface S closed by a curve C, can be calculated as

$$\Phi = \iint_S \mathrm{B} \cdot dS = \iint_S (\nabla \mathrm{xA}) \cdot dS = \oint_C A \cdot dl \quad (11)$$

Where B is the magnetic flux density, and A is the magnetic vector potential.

Replacing (11) in (10):

$$V = -N_R j\omega \iint_S \mathrm{B} \cdot dS \quad (12)$$

or

$$V = -N_R j\omega \oint_C A \cdot dl \quad (13)$$

Given that the FEM simulator allows to calculate B or A, it can be used any of these equations to define which surface S or curve C make for the greatest induced voltage.

To do this, it is used the equation (13) with $N_R = 1$. Using the FEM simulator, it is calculated the magnetic vector potential induced by the buried metal (Fig.20–Fig.21), and the numerical integration over C is done. In this case the transmitter and receiver position is X=0,01 m.

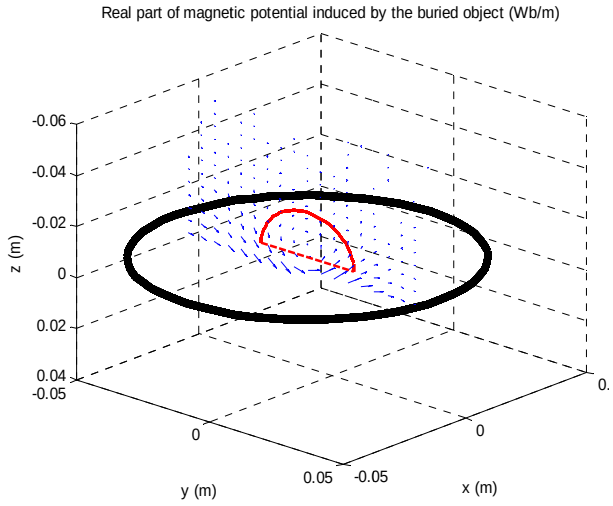

Fig.20. Real part of the magnetic vector potential induced by the buried metal in plane X=0,01 m

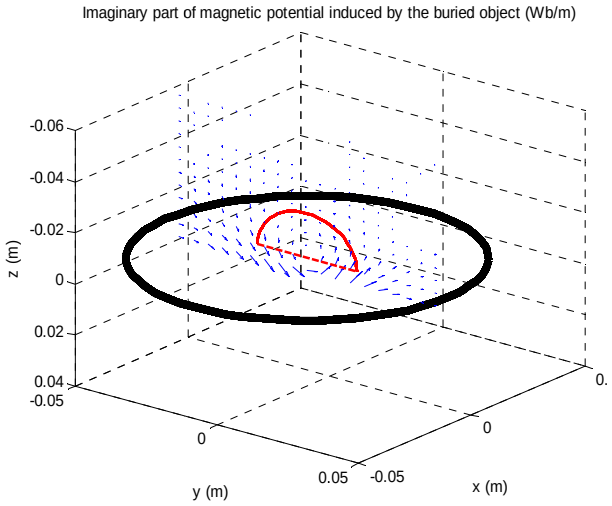

Fig.21. Imaginary part of the magnetic vector potential induced by the buried metal in plane X=0,01 m.

Initially, it is analyzed the rectangular receiver coil, for this geometry it is needed to determine the width and high of the rectangular coil to get the greatest induced voltage. To do so, it is necessary to calculate the magnetic vector potential over the line that forms the rectangle (Fig22–Fig23), and doing the integration of the equation (13) numerically as a sum of the potential in many points separatedΔl.

$$\oint_C A \cdot dl = \sum A(l) \cdot \Delta l \qquad (14)$$

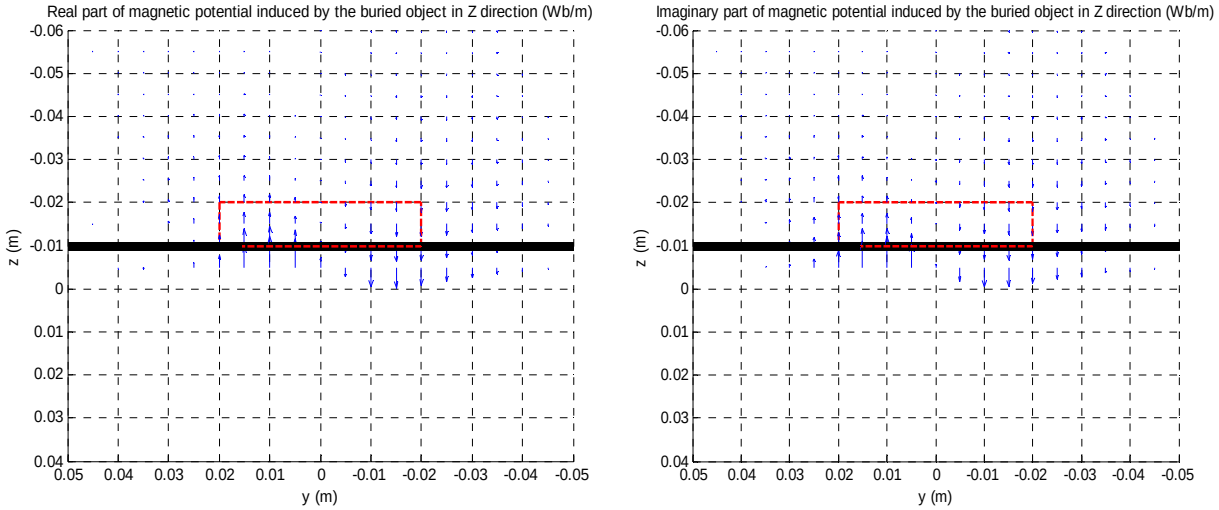

Fig22. Real and imaginary part of the magnetic vector potential induced in Z direction by the buried metal in plane X=0,01 m.

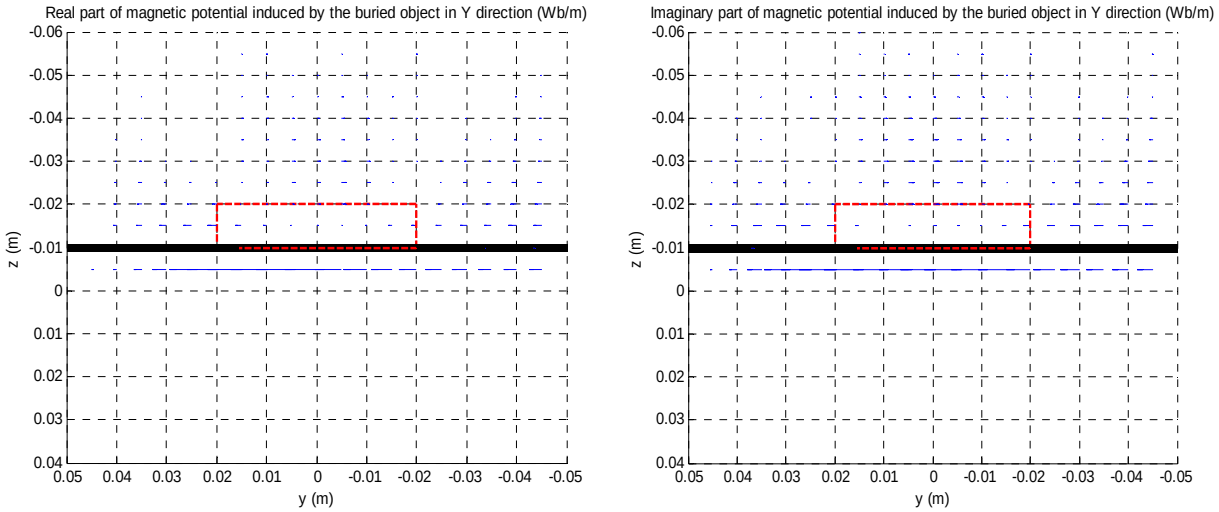

Fig23. Real and imaginary part of the magnetic vector potential induced in Y direction by the buried metal in plane X=0,01 m.

In order to get results with a higher resolution (*smaller* Δl), it was used a 2D interpolation to obtain the potential A, at any position in the simulation scenario (Fig24), this allows to calculate the voltage induced in a coil of any shape.

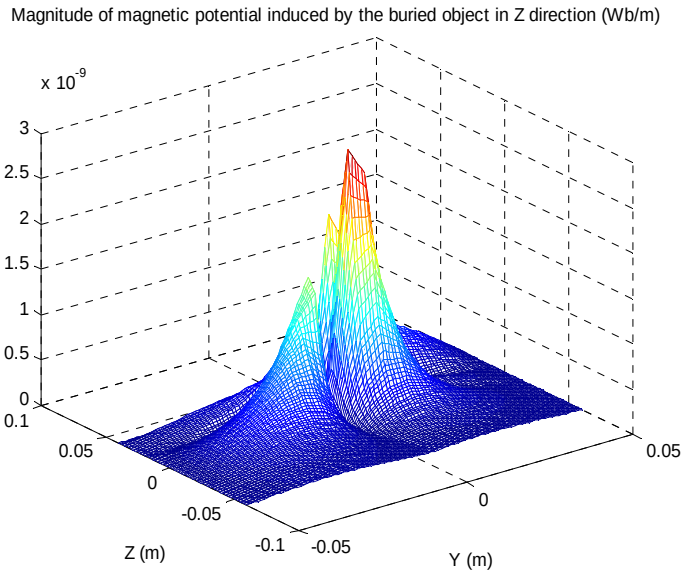

Fig24. Magnitude of the magnetic vector potential induced in Z direction.

Fig25shows, the magnitude of the induced voltage in a rectangular coil calculated with (13), as a function of this coil width and height. According to this results, the greatest induced voltage is obtained when the coil width is around 9 cm (Fig26), whereas the coil height does not seem to be very influent (Fig27).

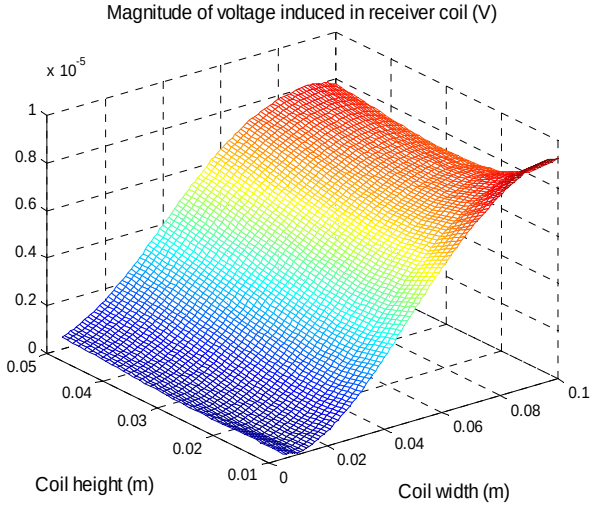

Fig25Magnitude of the induced voltage in a rectangular coil as a function of the coil width and height.

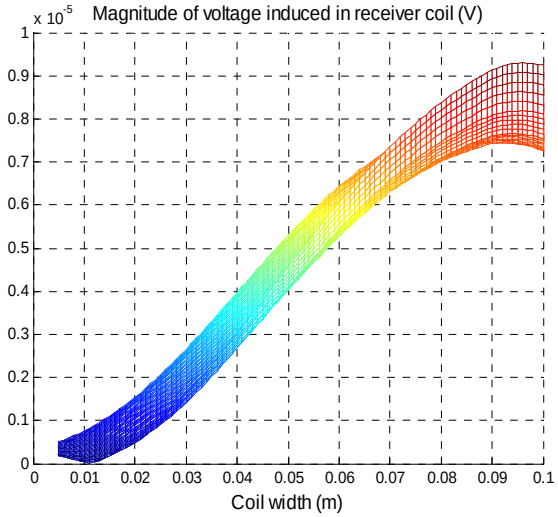

Fig26 Coil width vs magnitude of induced voltage.

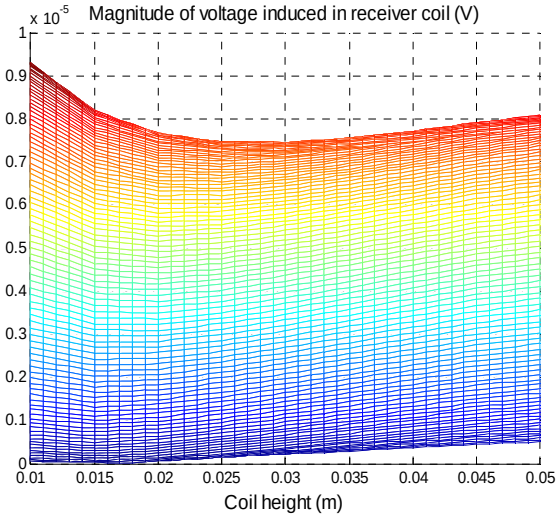

Fig27. Coil height vs magnitude of induced voltage.

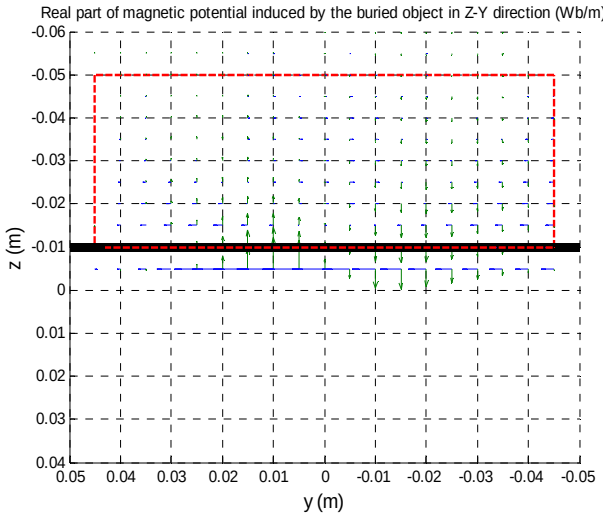

Fig28. Ideal size of the rectangular receiver coil of a detector that senses the induced magnetic field in X direction.

With a procedure similar to the above, a semicircular receiver coil was analyzed; in this case, it is needed to calculate A in ϕ direction at many points of the semicircle, and on the bottom part of the coil it is enough to calculate A in Y direction. To calculate A in ϕ direction, it is needed to do a coordinate transformation (15).

$$A_\phi = A_y(-sin(\phi)) + A_z(cos(\phi)) \quad (15)$$

By doing numerical integration, were obtained the results fromFig29, and it can be concluded that the greatest induced voltage is obtained when the semicircle radius is around 4.5 cm.

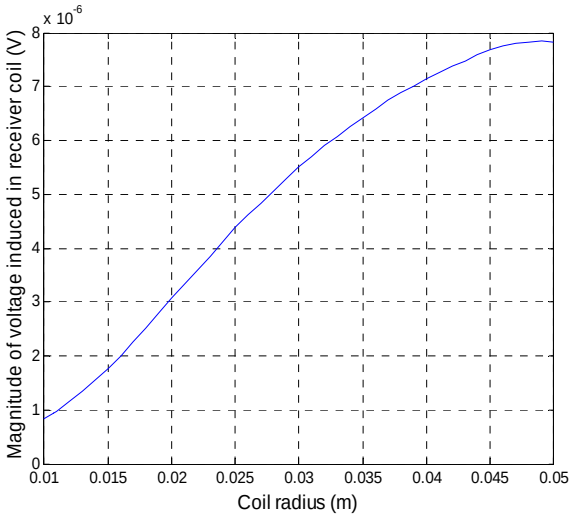

Fig29. Semicircle radius vs magnitude of induced voltage.

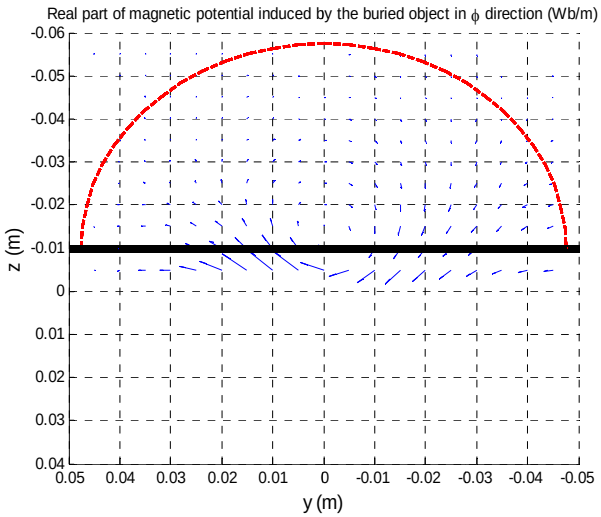

Fig30. Ideal size of the semicircular receiver coil of a detector that senses the induced magnetic field in direction X.

By comparing the results obtained with the rectangular and semicircular coil, it can be seen that the maximum induced voltage is similar in both cases ($around 8\ X\ 10^{-6}\ V$). Therefore, any of the geometries can be chosen. It is important to remember that the transmitter and receiver number of spires is 1 in the simulations, and these values scale the induced voltage in the receiver; consequently, if the receiver coil number of spires is 20, and the transmitter number of spires is also 20, the induced voltage will be 400 times greater.

Evidently, the sensitivity of the proposed detector is lesser than the sensitivity of a detector that measures the induced magnetic field in Z direction. However, the sensitivity can be easily improved by increasing the current that powers the transmitter coil, but solving the problems produced by the soil and the transmitter coil in a detector that measures the magnetic field in Z direction, requires complex solutions that involve hardware and software, increasing the device probability of failure.

According to the experiments done in [1], magnetic soils are the biggest challenge for metal detectors used in demining, given that the proposed detector does not sense the magnetic field induced by the soil, this detector takes advantage of magnetic and conductive soils, due that the magnetic field induced by buried objects increases in this kind of soils, as can be seen in [5].

The proposed system can be used as metal detector; however, it could be part of a more complex system which includes for example a traditional high sensitivity sensor of magnetic field in Z direction (Fig31). This system could measure magnetic field in Z and X direction, and determine the presence of a buried metallic target when both sensors detect the change in the magnetic field, by this way, it can be guaranteed that the buried object is indeed metallic; whereas if it is only sensed a magnetic field in Z direction, and nothing is sensed in X direction, the alarm could be due to the soil.

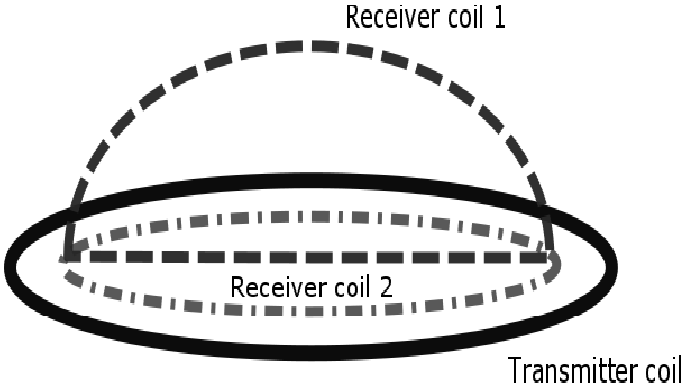

Fig31. Metal detector that senses magnetic field in X and Z direction.

IV. CONCLUSIONS

This investigation proposes a novel design of metal detector for humanitarian demining based on simulations made with numerical and analytical models.

The main objective of the proposed design is minimizing the effect of the soil in the detector performance, which is currently a known important problem in demining.

By using numerical and analytical modeling, is possible to determine that the electromagnetics properties of the soil are highly influentialin the performance of the metal detector.

According to the experiments carried out, magnetic soils represent the greatest challenge for the metal detectors used in demining, since in the proposed detector the field induced by the ground is not measured, it is taking advantage of the magnetic and conductive soils, since the field induced by buried objects increases in this type of soil

Additionally, this detector avoids the magnetic field induced directly by the transmitter coil. To do this, a receiver in quadrature with the transmitter was proposed, and it was probed that this configuration could detect metal buried objects. The dimensions of the receiver were defined, in order to guarantee the maximum magnitude of induced voltage.

REFERENCES

[1] K. Takahashi, H. Preetz y J. Igel, «Soil properties and performance of landmine detection by metal detector and ground-penetrating radar—soil characterisation and its verification by a field test,» Journal of Applied Geophysics, vol. 73, pp. 368-377, 2011.
[2] Y. Das, «Effects of Soil Electromagnetic Properties on Metal Detectors,» IEEE Transactions on Geoscience and Remote Sensing, vol. 44, nº 6, pp. 1444-1453, Junio 2006.
[3] Y. Das, «A preliminary investigation of the effects of soil electromagnetic properties on metal detectors.,» Proc. SPIE, p. 677–690, 2004.
[4] C. Bruschini, «On the low-frequency EMI response of coincident loops over a conductive and permeable soil and corresponding background reduction schemes,» Geoscience and Remote Sensing, IEEE Transactions on, vol. 42, nº 8, pp. 1706-1719, 2004.
[5] J. F. Vargas Buitrago, R. Bustamante Miller y M. E. Everett, «Modeling of Demining Scenarios Using Metal Detectors,» International Journal of Engineering and Technology, vol. 6, nº 4, pp. 1683-1696, 2014.
[6] S. Mukherjee y M. E. Everett, «3D controlled-source electromagnetic edge-based finite element modeling,» GEOPHYSICS, vol. 76, nº 4, p. F215–F226, 2011.